PROCEEDINGS OF SCIENCE

SIDIS Pion Beam Spin Asymmetries with CLAS 12 at 10.6 GeV

Stefan Diehl
Justsus Liebig University Giessen
Heinrich-Buff-Ring 16, 35392 Giessen, Germany
University of Connecticut
Storrs, Connecticut 06269, USA
E-mail: stefan.diehl@exp2.physik.uni-giessen.de

for the CLAS collaboration

The CLAS12 detector at Jefferson Laboratory (JLab) started data taking with a polarized 10.6 GeV electron beam, interacting with an unpolarized liquid hydrogen target in February 2018. One of the first quantities which could be extracted from the new data is the moment $A_{LU}^{\sin(\phi)}$ corresponding to the polarized electron beam spin asymmetry in semi-inclusive deep inelastic scattering. $A_{LU}^{\sin(\phi)}$ is a twist-3 quantity which provides information about the quark gluon correlations in the nucleon. The paper will present a simultaneous study of all three pion channels (π^+, π^0 and π^-) over a large kinematic range with virtualities Q^2 ranging from 1 GeV² up to 8 GeV². Preliminary results for the measurement in a large range of z, x_B, P_T and Q^2, including up to now not measured kinematic regions will be presented.

XXVII International Workshop on Deep-Inelastic Scattering and Related Subjects - DIS2019
8-12 April, 2019
Torino, Italy

PoS(DIS2019)173

1. Introduction and Motivation

To obtain a deeper understanding of the origin of the proton spin, the focus of the hadron physics community has moved beyond the collinear PDFs towards the study of the partons motion and its spatial distribution in the transverse plane, perpendicular to the momentum of the parent hadron. To describe these distributions, two sets of non-perturbative functions have been introduced. On the one side, Transverse-momentum-dependent parton distributions (TMDs) are used to describe the longitudinal and transverse momentum distributions. On the other side, Generalized parton distributions (GPDs) are used to describe the longitudinal momentum distributions and the transverse positions of the hadrons.

The production of pions in semi inclusive deep inelastic electron scattering (SIDIS) is an important tool to study the TMD of partons. The diagram in fig. 1 shows the SIDIS scattering process including the involved parton distribution (PDF) and fragmentation function (FF). In a single photon exchange model, the differential cross section of this process can be written as a product of leptonic ($L_{\mu\nu}$) and hadronic ($2MW_{\mu\nu}$) tensors [1].

$$\frac{d\sigma}{dx_B dz dy d^2P_T} = \frac{\pi\alpha^2 yz}{2Q^4} \mathcal{L}_{\mu\nu} 2MW^{\mu\nu} \tag{1}$$

With the fraction of the protons momentum carried by the struck quark x_B, the energy fraction of the incoming lepton carried by the virtual photon y, the energy fraction of the virtual photon carried by the outing hadron z, the transverse momentum of the final state hadron P_T and the virtuality Q^2 of the collision. For the special case of a polarized electron beam, interacting with an un-polarized target, the cross section is given by [2]:

$$\frac{d\sigma}{dx_B\, dQ^2\, dz\, d\phi_h\, dp_{h\perp}^2} = K(x,y,Q^2)\Big\{F_{UU,T} + \varepsilon F_{UU,L} + \sqrt{2\,\varepsilon(1+\varepsilon)}\cos\phi_h F_{UU}^{\cos\phi_h} + \varepsilon\cos(2\phi_h) F_{UU}^{\cos 2\phi_h} + \lambda_e\sqrt{2\,\varepsilon(1-\varepsilon)}\sin\phi_h F_{LU}^{\sin\phi_h}\Big\} \tag{2}$$

It consists of different structure functions F_{UU} and F_{LU} and depends on the azimuthal angle ϕ between the electron scattering plane and the hadron production plane as shown in fig. 2, according to the definition of the trento convention [3].

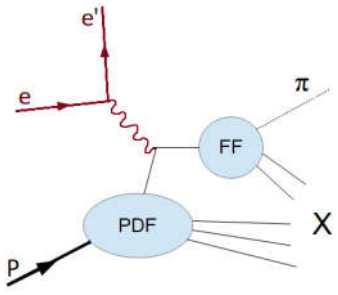

Fig. 1 Diagram of the SIDIS scattering process including the involved parton distribution (PDF) and fragmentation function (FF).

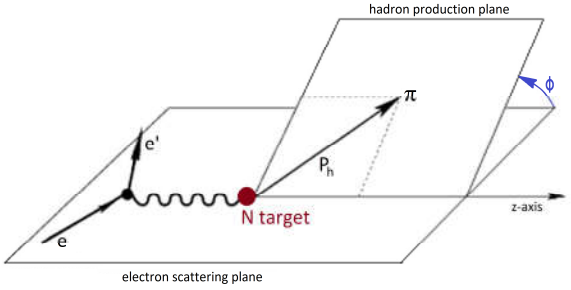

Fig. 2 Schematic drawing of the electron scattering and hadron production plane and definition of the azimuthal angle Φ between the two planes in the target rest frame.

This study will focus on the structure function $F_{LU}^{\sin(\phi)}$, which is related to the quark-gluon-quark correlations in the proton. Theoretically it can be expressed as a convolution of distribution and fragmentation functions [4, 5]:

$$F_{LU}^{\sin\phi} = \frac{2M}{Q}\mathcal{C}\left(-\frac{\hat{\mathbf{h}}\cdot\mathbf{k_T}}{M_h}\left(xeH_1^{\perp}+\frac{M_h}{M}f_1\frac{\tilde{G}^{\perp}}{z}\right)+\frac{\hat{\mathbf{h}}\cdot\mathbf{p_T}}{M}\left(xg^{\perp}D_1+\frac{M_h}{M}h_1^{\perp}\frac{\tilde{E}}{z}\right)\right)$$

twist-3 pdf; Collins FF; unpolarized dist. function; twist-3 FF; twist-3 t-odd dist. funcion; Boer-Mulders; twist-3 FF

(3)

The expression shows, that all parts contain a twist-3 component. Of special interest are the Boer-Mulders function $h_1^{\perp}$, which is a leading-twist time-reversal-odd TMD as well as $g^{\perp}$, a twist-3 time-reversal-odd TMD, which can be seen as the higher twist counter part of the Sivers function. The chiral-odd twist-3 PDF *e(x)* is expected to be related to the transverse force acting on the transversely polarized quarks in an unpolarized nucleon.

Even this structure function has been studied with several experiments like CLAS [1], HERMES [6] and COMPASS [7] during the recent years, there is still no consistent understanding of the contribution of each part to the total structure function. One reason for this can be seen in the low statistics and the resulting high error bars of many previous studies. In addition, due to the limited statistics all previous studies were binned in only one kinematic variable at a time, which introduces additional uncertainties for the extraction of theoretical information. The high statistics, which has been already collected and which will be collected with CLAS12 will enable a fully differential analysis for the first time and therefore provide excellent data for a deeper understanding of the single functions.

2. Experimental setup

The measurement presented in this work has been performed at Jefferson Laboratory, Newport News, Virginia, using a 10.6 GeV polarized electron beam, interacting with an unpolarized liquid hydrogen target during the first part of the RG-A run period from February to May 2018. The electron beam was provided by the Continuous Electron Beam Accelerator Facility (CEBAF), consisting of two linear accelerator sections and two regions with bending magnets. The electron helicity was flipped periodically with a frequency of 33 Hz which provides a practically equal luminosity for both helicity states. To further minimize systematic effects, a half wave plate was used to switch the definition of positive and negative helicity periodically for certain run periods. The beam polarization was measured regularly with a Møller polarimeter. The average value of the beam polarization has been determined to 0.850 ± 0.015. The measurements were performed with the upgraded CEBAF Large Acceptance Spectrometer (CLAS12). The CLAS12 detector setup, shown in fig. 3, consists of a central detector, surrounding the liquid hydrogen target cell and a dedicated forward detector. The forward detector starts with a high threshold cherenkov counter, which is used as a trigger for electrons. The tracking is provided by a torus magnet and a drift chamber system with 3 regions before, inside and after the magnet coils. The torus coils split the detector in 6 independent sectors. A low threshold cherenkov counter (4 sectors) and a RICH detector (1 sector) can be used for particle identification in addition to the forward time of flight system.

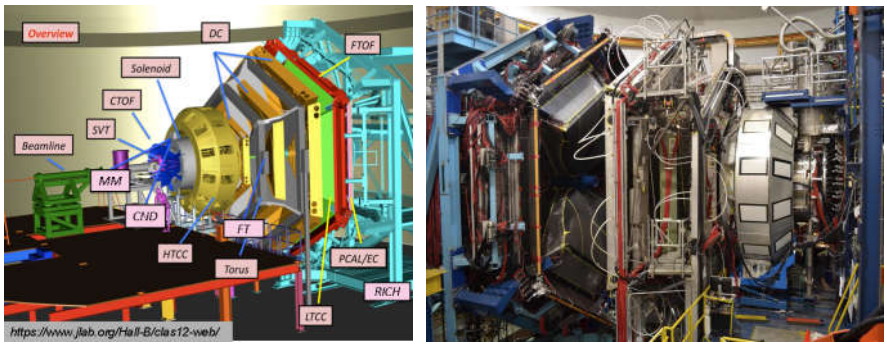

Fig. 3 Schematic drawing of the CLAS12 detector with the single sub-systems (left) and photograph of the real detector setup in hall B at JLAB (right)

Finally an electromagnetic calorimeter is used for the detection and identification of electrons and photons. The central detector is equipped with a solenoid magnet, a micromegas and a barrel silicon tracker as well as a central time-of-flight system and a neutron detector. To extend the detector coverage to small Q^2, a forward tagger, consisting of a tracker, a hodoscope and an electromagnetic calorimeter can be added in the most forward region around the beam-line.

3. Particle Identification and kinematic coverage

For semi-inclusive reactions, a clean particle identification if a key requirement, since no additional selection cuts are applied. For the identification of electrons, a series of cuts, mainly based on the electromagnetic calorimeter is applied. The electromagnetic calorimeter of CLAS consist of 3 regions, a preshow calorimeter (PCAL), followed by an inner and outer electromagnetic calorimeter. Each region is a sampling structure of lead and organic scintillator bars or fibers. The following cuts are applied:

- Fiducial cuts for the 3 drift-chamber regions
- Fiducial cuts for the pre-shower calorimeter.
- A minimal energy deposition in the PCAL to reject pions, which due to their minimal ionizing nature deposit less energy than electrons in this region.
- A calorimeter sampling fraction cut, adjusted to the 3σ region of the total electron sampling fraction to reject pions and electronic noise.
- A cut on the z-vertex position

For the identification of photons used for the π^0 reconstruction, first a fiducial cut on the PCAL is applied. The separation from neutrons is then done via the time of flight information from the calorimeter. For the charged pions, fiducial cuts on the 3 regions of the drift-chambers are applied. After this, a maximum likelihood estimation based on β versus p with a 3σ confidence level has been used for the separation from protons and kaons. The beta versus p distribution for positive hadrons in the forward detector is shown in fig. 6. The neutral pions have been reconstructed from all permutations of photon pairs with an energy threshold of 400 MeV for each photon. The π^0 peak in the invariant two photon mass (fig. 7) shows a resolution σ of 10.5 MeV. To obtain a clean data sample kinematic cuts have been placed on the electrons and pions. The minimal energy for electron and pions has been set to 1.5 GeV. The maximum pion energy is 9.0 GeV. The θ angle of pions is limited between 5° and 90°. To remove the target fragmentation region and to reject contributions from exclusive channels, z has been limited between 0.2 and 0.7 for plots in which no z dependence is involved.

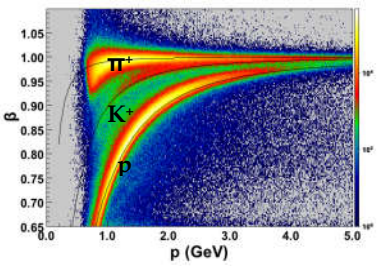

Fig. 6 Correlation between β and momentum for positive hadrons.

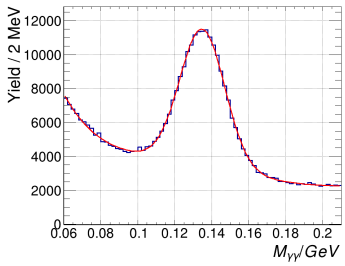

Fig. 7 π^0 peak in the two photon invariant mass.

The kinematic coverage of CLAS12 reaches in Q^2 up to 12 GeV² and in W up to 4 GeV. In x_B the region between 0.05 and 1 can be covered, while in P_T a reasonable statistics is available up to 1.5 GeV. Fig. 8 shows the correlation between Q^2, W and x_B.

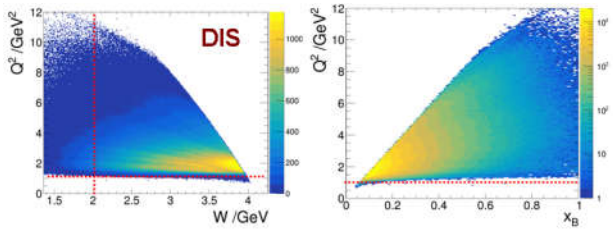

Fig. 8 Correlation between Q^2 and W (left) and Q^2 and x_B (right).

4. Analysis procedure and results

The cross section introduced in equation (2) can be expressed with the three moments $A_{UU}^{\cos(\phi)}$, $A_{UU}^{\cos(2\phi)}$ and $A_{LU}^{\sin(\phi)}$ as:

$$d\sigma = d\sigma_0\left(1 + A_{UU}^{\cos\phi}\cos\phi + A_{UU}^{\cos 2\phi}\cos 2\phi + \lambda_e A_{LU}^{\sin\phi}\sin\phi\right) \tag{4}$$

Based on this expression, the beam spin asymmetry can be defined as:

$$BSA = \frac{d\sigma^+ - d\sigma^-}{d\sigma^+ + d\sigma^-} = \frac{A_{LU}^{\sin\phi}\sin\phi}{1 + A_{UU}^{\cos\phi}\cos\phi + A_{UU}^{\cos(2\phi)}\cos(2\phi)} \tag{5}$$

If the beam-spin asymmetry is plotted as a function of ϕ (fig. 9), a good agreement with a sinoid shape can be observed for all 3 pions. It has to be noted, that the present analysis is based on only 2% of the approved beam time and no systematic uncertainties are studied yet. Since the contributions of $A_{UU}^{\cos(\phi)}$ and $A_{UU}^{\cos(2\phi)}$ are obviously small, a fit with the function $A_{LU}^{\sin(\phi)}\cdot\sin(\phi)$ can be performed, which provides the moment $A_{LU}^{\sin(\phi)}$, which is directly correlated to $F_{LU}^{\sin(\phi)}$. The fit has been performed in different bins in z, x_B, P_T and Q^2, with the results for $A_{LU}^{\sin(\phi)}$ shown in fig. 10.

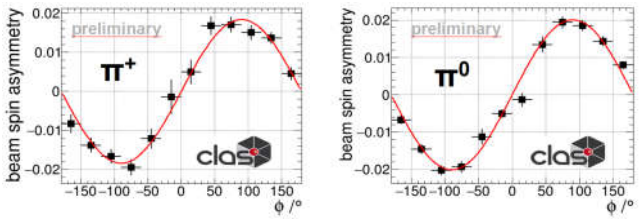

Fig. 9 Beam spin asymmetry as a function of ϕ for π^+ (left) and π^0 (right), integrated over all kinematic variables. The red line shows the fitted sin(ϕ) dependence.

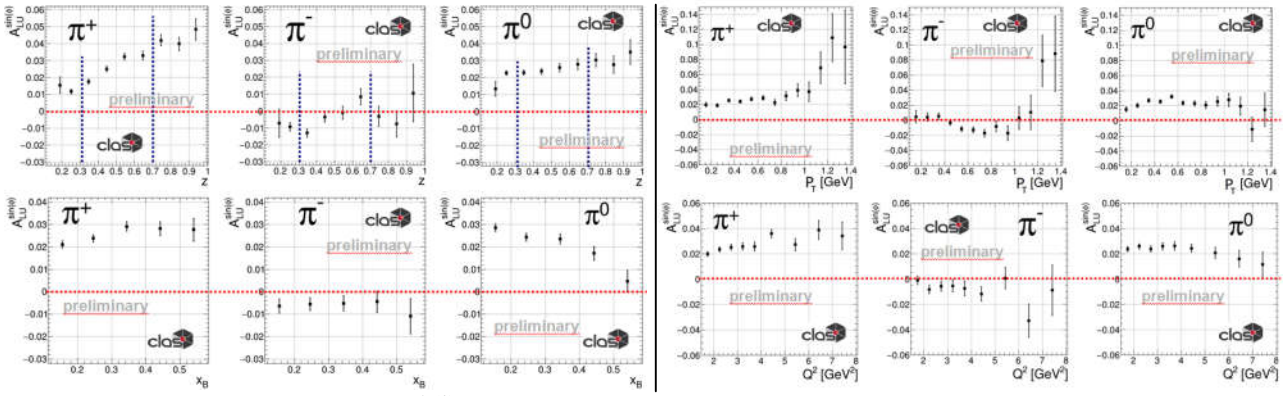

Fig. 10 Preliminary result for $A_{LU}^{\sin(\phi)}$ binned in in z (left, upper row), x_B (left, lower row), P_T (right, upper row) and Q^2 (right, lower row) for π^+ (left), π^- (centre) and π^0 (right). The dashed blue lines in z provide the cut borders which are applied for all other variables.

It can be observed, that π^+ and π^0 provide a positive $A_{LU}^{\sin(\phi)}$ value, while $A_{LU}^{\sin(\phi)}$ is zero or slightly negative for π^-. This is consistent with the results of previous experiments. A great advantage of the CLAS12 dataset is besides the possibility of a multi-dimensional binning, also the extension of the kinematic coverage in Q^2 and P_T. Especially Q^2 which was limited to 4 GeV^2 in the previous CLAS analyses can now be extended to 8 GeV^2 or even above with reasonable statistical uncertainties, which will provide valuable new insights into the Q^2 evolution of the structure function.

5. Conclusion and Outlook

Even with a small sub-sample of only around 4 % of the already recorded statistics (2% of the approved beam time), a statistical uncertainty at the level of the full CLAS statistics at 6 GeV can be achieved in a one-dimensional binning. Based on this promising result, a fully differential analysis is planed with the full data-set. In addition, the presented results contain no study of the systematic uncertainty, which becomes very important when the statistical uncertainty is mall. Especially possible acceptance effects have to be studied in more detail.

Acknowledgements

We acknowledge the outstanding efforts of the staff of the Accelerator and the Physics Divisions at Jefferson Lab in making this experiment possible. The work is supported by DOE grant no: DE-FG02-04ER41309.

References

[1] W. Gohn, H. Avakian, K. Joo, M. Ungaro et al., Phys. Rev. D 89, 072011 (2014)
[2] Alessandro Bacchetta, Markus Diehl, Klaus Goeke et al., JHEP 0702, 093 (2007).
[3] A. Bacchetta, U. D'Alesio, M. Diehl, and C. A. Miller, Phys. Rev. D 70, 117504 (2004).
[4] A. Bacchetta, M. Diehl, K. Goeke et al., J. High Energy Phys. 02, 093 (2007).
[5] J. Levelt and P. J. Mulders, Phys. Lett. B 338, 357 (1994).
[6] A. Airapetian, Z. Akopov, M. Amarian, et al. (HERMES collab.), Phys. Let. B 648, 164–170 (2007).
[7] C. Adolph, R. Akhunzyanov et al. (COMPASS collab.), Nucl. Phys. B 886, 1046–1077 (2014).